Spin manipulating stored 1.85 GeV/c vector and tensor polarized spin-1 bosons

V. S. Morozov, A. D. Krisch, M. A. Leonova, R. S. Raymond, D. W. Sivers, and V. K. Wong
Spin Physics Center, University of Michigan, Ann Arbor, Michigan 48109-1120, USA

R. Gebel, A. Lehrach, B. Lorentz, R. Maier, D. Prasuhn, A. Schnase, and H. Stockhorst
Forschungszentrum Jülich, Institut für Kernphysik, Postfach 1913, D-52425 Jülich, Germany

D. Eversheim, F. Hinterberger, H. Rohdjeß, and K. Ulbrich
Helmholtz-Institut für Strahlen- und Kernphysik, Universität Bonn, D-53115 Bonn, Germany

K. Yonehara
Department of Biological, Chemical, and Physical Sciences, Illinois Institute of Technology, Chicago, Illinois 60616, USA
(Received 1 February 2005; published 3 June 2005)

We recently studied the spin manipulation of 1.85 GeV/c vertically polarized deuterons stored in the COSY cooler synchrotron. We adiabatically swept an rf dipole's frequency through an rf-induced spin resonance and observed its effect on the deuterons' vector and tensor polarizations. After optimizing the resonance crossing rate and maximizing the rf dipole's voltage, we measured spin-flip efficiencies of $97 \pm 1\%$ and $98.5 \pm 0.3\%$ in two separate runs. We also confirmed at higher energy the striking behavior of the spin-1 tensor polarization recently found at IUCF.

DOI: 10.1103/PhysRevSTAB.8.061001 PACS numbers: 29.27.Bd, 29.27.Hj, 41.75.Ak

I. INTRODUCTION

Many polarized beam experiments are now operating in storage rings such as the MIT-Bates storage ring [1], COSY [2], RHIC at Brookhaven [3] and HERA at DESY [4,5]. Frequent spin direction reversals can significantly reduce the systematic errors in such spin asymmetry measurements. Beams of spin-$\frac{1}{2}$ particles have been successfully spin flipped: horizontally polarized electrons at the MIT-Bates storage ring [6], and horizontally and vertically polarized protons at the IUCF cooler ring [7–13] and COSY [14]. Stored spin-1 deuterons were also spin flipped at the IUCF cooler ring [15]. We recently extended the studies of their interesting behavior by spin flipping 1.85 GeV/c vector and tensor polarized deuterons stored in the COSY cooler synchrotron.

A beam of spin-1 bosons has a more complex polarization behavior than spin-$\frac{1}{2}$ fermions; their spin component, m, along the vertical axis can have three values: $m = +1, 0, -1$. Describing the polarization of a beam of spin-1 particles requires three vector polarization components and five independent second-rank tensor components [16,17]. The magnitudes of a vertically polarized beam's vector and tensor polarizations are given by [16]:

$$P_V \equiv (N_+ - N_-)/N; \qquad P_T \equiv 1 - 3(N_0/N), \tag{1}$$

where N_+, N_0, and N_- are the number of particles in $m = +1$, 0, and -1 states, respectively, and $N = N_+ + N_0 + N_-$ is the total number of particles.

In any flat circular accelerator or storage ring, with no horizontal magnetic fields, each deuteron's spin precesses around the vertical fields of the ring's bending magnets. The spin tune ν_s, which is the number of spin precessions during one turn around the ring, is proportional to the deuteron's energy

$$\nu_s = G\gamma, \tag{2}$$

where $G = (g - 2)/2 = -0.142\,987$ is the deuteron's gyromagnetic anomaly and γ is its Lorentz energy factor.

The deuteron's polarization can be perturbed by the horizontal rf magnetic field from either an rf solenoid or an rf dipole. At a resonant frequency the perturbations can add coherently to induce an rf spin resonance, which can flip the spin of stored polarized particles [7–14,18], such as deuterons [15]. The rf-induced spin resonance's frequency is

$$f_r = f_c(k \pm \nu_s), \tag{3}$$

where f_c is the deuterons' circulation frequency and k is an integer. Adiabatically ramping the rf magnet's frequency through f_r can rotate the deuterons' polarization direction by an angle θ around a horizontal axis. Under this rotation, the spin-1 vector and tensor polarizations, P_V and P_T (sometimes called P_z and P_{zz} [15]), respectively, transform as

$$P_V(\theta) = P_V^i \cos\theta, \qquad P_T(\theta) = P_T^i\left[\frac{3}{2}\cos^2\theta - \frac{1}{2}\right], \tag{4}$$

where P_V^i and P_T^i are the initial vector and tensor polarizations, respectively. When $\theta = \pi$ there is a vector spin flip: $P_V(\pi) = -P_V^i$; while the tensor polarization is unchanged $P_T(\pi) = P_T^i$. At mid-spin-flip, when $\theta = \frac{\pi}{2}$, note that $P_V(\frac{\pi}{2}) = 0$ while $P_T(\frac{\pi}{2}) = -\frac{1}{2}P_T^i$.

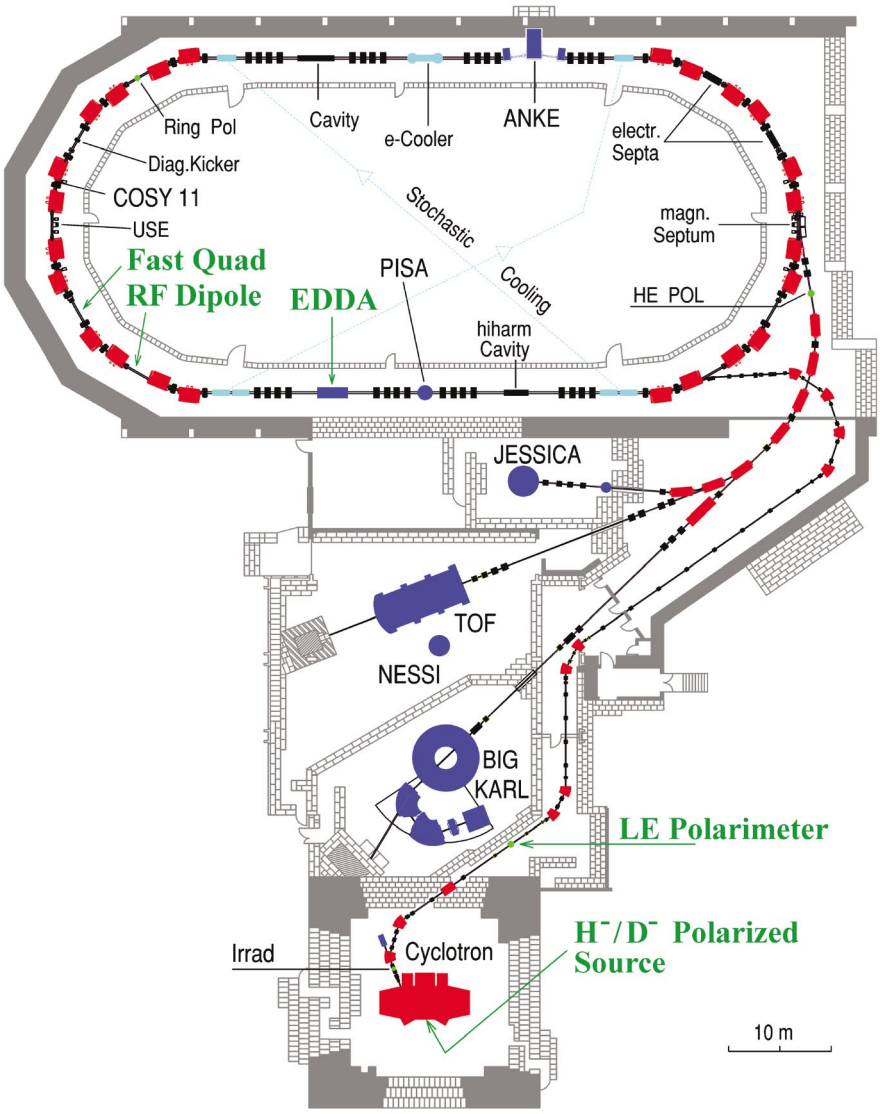

FIG. 1. (Color) Layout of the COSY storage ring, with its injector cyclotron and polarized ion source. Also shown are the rf dipole, the EDDA detector, and the low energy polarimeter.

The Froissart-Stora equation [19] relates the beam's vector polarization P_V, after ramping an rf dipole's frequency through a resonance, to the beam's initial vector polarization P_V^i and the ramp's frequency range Δf and ramp time Δt:

$$P_V = P_V^i \left\{ 2 \exp\left[\frac{-(\pi \epsilon f_c)^2}{\Delta f / \Delta t} \right] - 1 \right\}, \tag{5}$$

where $\Delta f / \Delta t$ is the resonance crossing speed. The resonance strength ϵ is given by [20]

$$\epsilon = \frac{1}{\pi \sqrt{2}} \frac{e(1 + G\gamma)}{p} \int B_{\mathrm{rms}} dl, \tag{6}$$

where e is the deuteron's charge, p is its momentum, and $\int B_{\mathrm{rms}} dl$ is the rf dipole's rms magnetic field integral.

II. APPARATUS

The apparatus used for this experiment, including the COSY storage ring [21–24], the EDDA detector [25], the low energy polarimeter, the injector cyclotron, and the polarized ion source [26–28] are indicated in Fig. 1, along with the rf dipole. The dipole consisted of an 8-turn ferrite-core copper coil with the spacing between its turns optimized to produce a uniform radial magnetic field; it was part of an LC resonant circuit, which normally ran at about 2.8 kV rms producing an $\int B_{\mathrm{rms}} dl$ of 0.54 ± 0.03 T mm at $f = 916$ kHz. Then using Eq. (6) for 1.85 GeV/c deuterons this gives a resonance strength

$$\epsilon = (16 \pm 1) \times 10^{-6}. \tag{7}$$

An air-core rf dipole at COSY was used earlier to spin-flip

polarized protons [14] and polarized deuterons [29] with lower spin-flip efficiency.

The beam emerging from the polarized D^- ion source was accelerated by the cyclotron to COSY's 75.6 MeV injection energy. Then the low energy (LE) polarimeter monitored the beam's polarization before injection into COSY to monitor the stable operation of the ion source and cyclotron. We measured the polarization in COSY using the EDDA detector [2,25] as a polarimeter. The beam parameters are given in the Table I.

TABLE I. COSY parameters for the December 2003 polarized deuteron experiment.

Parameter	Value
Circumference	183.4 m
Beam type	Polarized deuterons
Flattop momentum (p)	1.850 GeV/c
Flattop energy (γ)	1.4046
Circulation frequency (f_c)	1.147 430 MHz
Spin tune (ν_s)	−0.200 84
Momentum spread $(dp/p)_{\mathrm{rms}}$	5×10^{-4}
Horizontal emittance (ϵ_h)	7 mm mrad
Vertical emittance (ϵ_v)	<5 mm mrad
Max. beta-functions (H, V)	30 m in both planes
Max. dispersion function (H)	15 m
Horizontal betatron tune (ν_h)	3.62
Vertical betatron tune (ν_v)	3.60
H. chromaticity $\frac{(d\nu/\nu)_{h,v}}{(dp/p)}$	−2.6
V. chromaticity	0.2
Synchrotron tune (ν_{syn})	None: rf off on flattop
Transition energy (γ_{tr})	2.2
Transverse coupling	No skew-quads or solenoids
Cooling	Off
Orbit flatness (Δy_{max})	±5 mm
Mag. Align. error ($\Delta\theta_{\mathrm{max}}$)	<0.1 mrad
Injection momentum (p_i)	0.538 GeV/c
Acceleration rate (dp/dt)	1.15 (GeV/c) s^{-1}

III. POLARIMETER CALIBRATION

To reduce our systematic errors, we cycled the polarized source through the five vertical polarization states: $(P_V, P_T) = (0, 0), (-\frac{2}{3}, 0), (-\frac{1}{3}, -1), (-1, 1)$, and $(1, 1)$. The rf acceleration cavity was turned off and shorted during COSY's flattop; thus, there were no synchrotron sidebands [30–32]. The measured flattop polarization, before spin manipulation, was typically about 70%.

The deuteron vector and tensor polarizations were obtained using the EDDA detector. No published data were available at 1850 MeV/c for the vector and tensor analyzing powers of p-d elastic scattering; thus, they were determined in an earlier calibration run [33], as described below. First one measured the deuteron vector and tensor polarizations both below and above the experimental energy, at 1042 and 2430 MeV/c, where the analyzing powers were published [34,35]. These measured polarizations agreed within errors. Thus, there was no depolarization during acceleration between 1042 and 2430 MeV/c, which includes 1850 MeV/c. These two polarization data sets were used to obtain the vector and tensor analyzing powers for p-d elastic scattering at 1850 MeV/c [33].

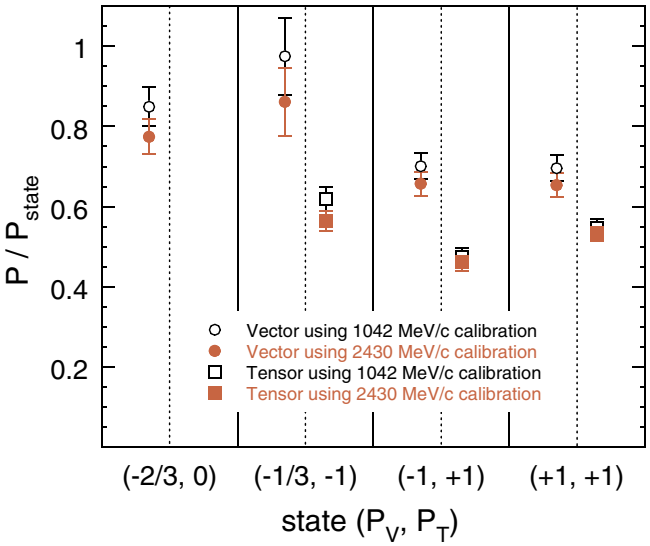

FIG. 2. (Color) Ratios of the vector and tensor deuteron polarizations to the ideal value of each polarization state from the source are plotted against the polarization state number for the 1850 MeV/c COSY deuteron beam. The open symbols indicate data points using the 1042 MeV/c calibration while the solid symbols indicate data using the 2430 MeV/c calibration.

We later used these elastic analyzing powers to measure the polarizations for each spin state as shown in Fig. 2. Note that the two polarizations obtained from the analyzing powers obtained from the 1042 MeV/c and the 2430 MeV/c calibrations agree within errors. We simultaneously calibrated the effective analyzing powers and detector efficiencies of the EDDA detector, which was at the same time operating as a simple 4-quadrant polarimeter using scalers to record all scattering events in each quadrant [33]. We also confirmed these calibrations to a precision of better than 1% during the main experiment [36]. We used these detector efficiencies and effective analyzing powers to obtain the vector and tensor polarizations from the measured scaler asymmetries during the main experiment.

IV. SPIN MANIPULATION

For each spin manipulation measurement in the main experiment, we linearly ramped, during 200 ms, the dipole's rf amplitude from about 0 to 2.8 kV rms producing an $\int B_{\mathrm{rms}} dl$ of about 0.54 T mm. We held this $\int B_{\mathrm{rms}} dl$

constant during the spin manipulation of a few seconds and then ramped it back to zero during 200 ms; then we inserted the EDDA target and measured the beam's vector and tensor polarizations.

The deuteron circulation frequency in the COSY ring was $f_c = 1.147\,43$ MHz at 1.850 GeV/c, where its Lorentz energy factor was $\gamma = 1.4046$. With these parameters, Eq. (2) gave a spin tune $\nu_s = G\gamma$ of -0.20084. Thus, at 1.850 GeV/c, Eq. (3) implies that the $k = 1$ depolarizing resonance's central frequency should occur at

$$f_r = (1 + G\gamma) f_c = 917.0 \text{ kHz}. \quad (8)$$

We first determined the approximate position of this spin depolarizing resonance by sweeping the rf dipole's frequency initially by ± 10 kHz around this f_r; then we continued by narrowing the frequency sweeping range into those half-ranges that caused spin flip. This technique was described earlier [6,12,13]. The resulting data indicated that the resonance was located near 916.9 kHz.

We then more precisely determined f_r by measuring the polarization, after running the rf dipole at different fixed frequencies near 916.9 kHz. The measured vector polarization ratios for the four nonzero polarization states are plotted against the rf dipole's frequency in Fig. 3. The P_V^i and P_T^i are the average of the six points furthest from the dip for each curve. The curve is a second-order Lorentzian fit which gave a central resonance frequency of $f_r = 916.962\,22 \pm 0.000\,26$ kHz and width of $w = 40.82 \pm 0.76$ Hz.

Figure 3 also shows similar tensor polarization data. The lower curve is a second-order Lorentzian fit to all states' tensor polarization ratios; the resonance's central frequency is $f_r = 916.9612 \pm 0.0025$ kHz, while its width is $w = 39.4 \pm 7.4$ Hz. Note that the f_r and w values obtained for the vector and tensor polarizations are both consistent.

We next maximized the deuteron polarization's spin-flip efficiency. We flipped them by linearly ramping the rf dipole's frequency from $f_r - 0.1$ to $f_r + 0.1$ kHz, with various ramp times Δt; we measured the polarizations after each frequency ramp. These measured vector and tensor polarizations are plotted against the ramp time in Fig. 4. The vector polarization data are fit to the empirically modified [6,11] Froissart-Stora formula [19]

$$\frac{P_V}{P_V^i} = -\eta_V = (1 + \eta_V^l) \exp\left[\frac{-(\pi \epsilon_V f_c)^2}{\Delta f/\Delta t}\right] - \eta_V^l, \quad (9)$$

where ϵ_V is the vector resonance strength. The parameter η_V^l is defined as the upper limit of the achievable spin-flip efficiency η_V when the exponential approaches zero. This limit could be due to many depolarizing mechanisms such as: Δf being too small to completely cover the resonance width, or any weak nearby resonance. This fit gave

$$\eta_V^l = 100.4 \pm 2.0\%, \quad \epsilon_V = (1.167 \pm 0.011) \times 10^{-6}. \quad (10)$$

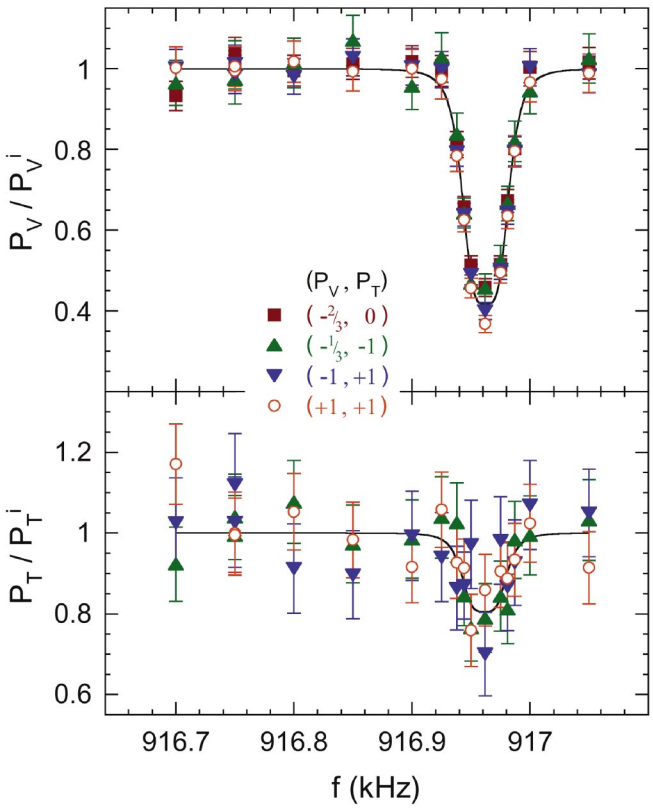

FIG. 3. (Color) The measured vector and tensor deuteron polarization ratios at 1850 MeV/c are plotted against the rf dipole's fixed frequency. The P_V^i and P_T^i are the average of the six points furthest from the deep for each curve. The rf dipole's $\int B_{\text{rms}} dl$ was 0.54 T mm. The curves are second-order Lorentzian fits.

To fit the tensor data in Fig. 4, we use Eqs. (4) and (9) as in [15] to obtain

$$P_T/P_T^i = \frac{3}{2}(P_V/P_V^i)^2 - \frac{1}{2} = \frac{3}{2}\left\{(1 + \eta_T^l)\exp\left[\frac{-(\pi \epsilon_T f_c)^2}{\Delta f/\Delta t}\right] - \eta_T^l\right\}^2 - \frac{1}{2}, \quad (11)$$

where we introduced η_T^l as the tensor spin-flip efficiency and ϵ_T as the tensor resonance strength. Fitting the tensor polarization data in Fig. 4 and averaging for the three states then gives

$$\eta_T^l = 100.2 \pm 2.1\%, \quad \epsilon_T = (1.144 \pm 0.022) \times 10^{-6}. \quad (12)$$

Note that the ϵ_V and ϵ_T obtained from the extended Froissart-Stora formula, Eqs. (9) and (11), agree quite well with each other. However, both are more than 10 times smaller than the ϵ obtained from the measured $\int B \cdot dl$ in Eq. (7). We recently started an experiment to try to understand the ϵ discrepancy [20].

For each of the three nonzero tensor polarization states, the two data points nearest the Δt value in Fig. 4 where $P_V = 0$ agree fairly well with the fit curves for the tensor ratio P_T/P_T^i. This agrees very well with the prediction of

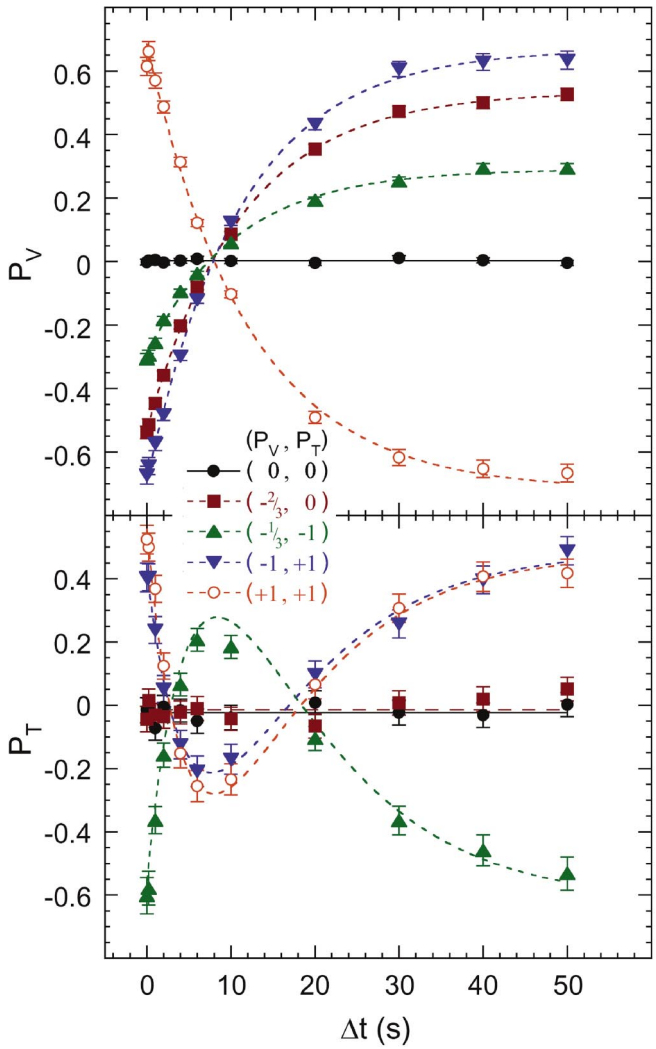

FIG. 4. (Color) The measured vector and tensor deuteron polarizations at 1850 MeV/c are plotted against the rf dipole ramp time Δt. The rf dipole's frequency half-range $\Delta f/2$ was 100 Hz, and its $\int B_{\rm rms} dl$ was 0.54 T mm. The top and bottom curves are fits using Eqs. (9) and (11), respectively.

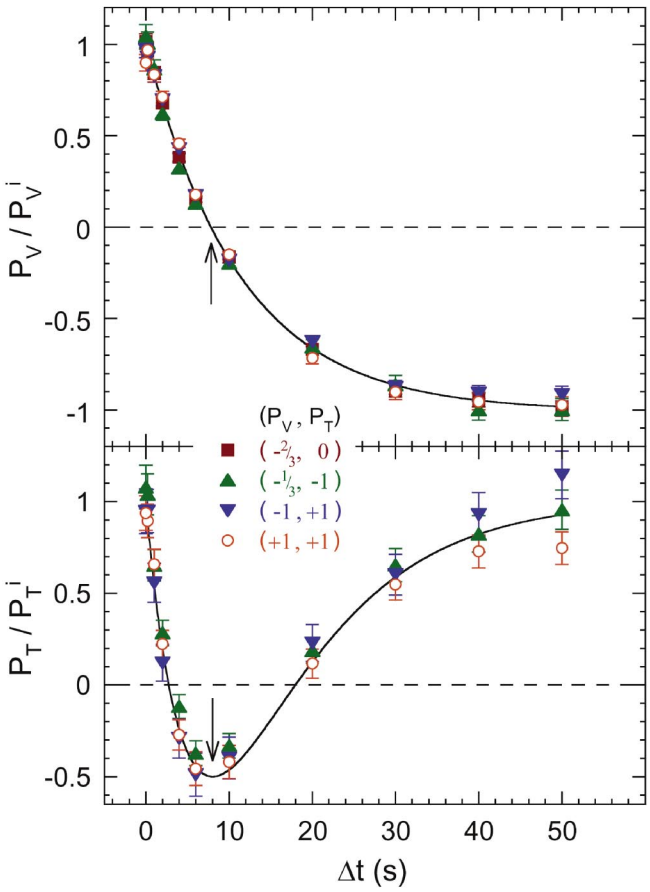

FIG. 5. (Color) The measured vector and tensor deuteron polarization ratios at 1850 MeV/c are plotted against the rf dipole ramp time Δt. The P_V^i and P_T^i were obtained from fits to the data as shown in Table II. The rf dipole's frequency half-range $\Delta f/2$ was 100 Hz, and its $\int B_{\rm rms} dl$ was 0.54 T mm. The top and bottom curves are fits to all states' data using Eqs. (9) and (11), respectively. The arrows mark a 90° rotation where $P_V = 0$ and $P_T = -\frac{1}{2} P_T^i$.

Eqs. (4) and (11) that P_T/P_T^i is $-\frac{1}{2}$ when $P_V = 0$. Moreover, the η and ϵ values shown in Eqs. (10) (vector) and (12) (tensor) are all consistent with each other. This confirms [15] that one η^l and one ϵ describe both the vector and tensor polarizations during a resonance crossing.

For the data in Fig. 4, we also calculated the ratios of the vector and tensor polarizations to their initial values obtained from the fits; these ratios are plotted against the frequency ramp time in Fig. 5 for the nonzero states. This allowed us to fit all nonzero vector and tensor data to Eqs. (9) and (11), respectively. Notice the good agreement of the data points for different states with each other and with the fit curves. Fitting the vector and tensor data sets, each with a single curve, gave a better precision results for η^l and ϵ than Eqs. (10) and (12)

$$\eta_V^l = 100.6 \pm 1.5\%, \quad \epsilon_V = (1.166 \pm 0.009) \times 10^{-6};$$
$$\eta_T^l = 100.2 \pm 1.8\%, \quad \epsilon_T = (1.152 \pm 0.022) \times 10^{-6}. \quad (13)$$

We next spin flipped the deuterons while varying the rf dipole's frequency range Δf, with its Δt at 50 s and its $\int B_{\rm rms} dl$ at 0.54 T mm. The data in Fig. 6 shows a broad maximum in the spin-flip efficiency near $\Delta f/2 = 75$ Hz. The Froissart-Stora equation is only valid for sufficiently wide frequency ranges covering the spin resonance completely; thus, in Fig. 6, we fit the vector and tensor data to Eqs. (9) and (11), respectively, only at $\Delta f/2 = 75$ Hz and above. The average vector and tensor fit results are

$$\eta_V^l = 96.8 \pm 2.9\%, \quad \epsilon_V = (1.165 \pm 0.014) \times 10^{-6};$$
$$\eta_T^l = 99.1 \pm 3.0\%, \quad \epsilon_T = (1.155 \pm 0.027) \times 10^{-6}. \quad (14)$$

TABLE II. Fit results for Figs. 4 and 5.

Vector and tensor fit results				
State	P_V^i	η_V	$\epsilon_V(\times 10^{-6})$	χ^2
$(-2/3, 0)$	-0.530 ± 0.010	1.01 ± 0.04	1.17 ± 0.02	4.5
$(-1/3, -1)$	-0.294 ± 0.008	0.99 ± 0.05	1.21 ± 0.03	9.3
$(-1, +1)$	-0.692 ± 0.014	0.97 ± 0.04	1.18 ± 0.02	6.6
$(+1, +1)$	0.684 ± 0.014	1.05 ± 0.04	1.13 ± 0.02	17.2
All states ($N - 2 = 42$)		1.006 ± 0.015	1.166 ± 0.009	46.0
State	P_T^i	η_T	$\epsilon_T(\times 10^{-6})$	χ^2
$(-1/3, -1)$	-0.56 ± 0.03	1.04 ± 0.04	1.12 ± 0.03	15.2
$(-1, +1)$	0.43 ± 0.03	1.05 ± 0.04	1.16 ± 0.05	3.0
$(+1, +1)$	0.56 ± 0.03	0.95 ± 0.03	1.18 ± 0.04	4.4
All states ($N - 2 = 31$)		1.002 ± 0.018	1.152 ± 0.022	29.9

Below $\Delta f/2 = 75$ Hz in Fig. 6, we used hand-drawn curves to guide the eye.

For the data in Fig. 6, we also calculated the ratios of the vector and tensor polarizations to their initial values obtained from the fits; these ratios are plotted against the frequency range in Fig. 7 for the nonzero states. Notice that the data points for different states agree with each other within errors. We again fit all nonzero vector and tensor data, at and above $\Delta f/2 = 75$ Hz, to Eqs. (9) and (11), respectively. These fits gave

$$\eta_V^l = 97.3 \pm 1.6\%, \quad \epsilon_V = (1.166 \pm 0.010) \times 10^{-6};$$
$$\eta_T^l = 98.8 \pm 2.0\%, \quad \epsilon_T = (1.156 \pm 0.027) \times 10^{-6}. \qquad (15)$$

We showed the fits as solid lines to compare the results of Eqs. (9) and (11) with the experimental data both above and below $\Delta f/2 = 75$ Hz. Notice that above $\Delta f/2 = 75$ Hz the vector data is described very well by Eq. (9) while below $\Delta f/2 = 75$ Hz the vector data's behavior (shown by the dashed curve) is very different from Eq. (9). However, the tensor data seem consistent with Eq. (11) for all frequency ranges.

A possible explanation for this behavior involves the beam's spin-resonance frequency spread due to its momentum spread. When the frequency range is smaller than the resonance frequency spread, only those particles, with resonance frequencies within the frequency range, are spin flipped according to the Froissart-Stora formula, while the rest of the beam's polarization remains unchanged. The beam's total polarization is the average polarization of the flipped and nonflipped parts. Below $\Delta f/2 = 75$ Hz, the vector and tensor polarizations of the flipped part are about $-P_V^i$ and P_T^i, respectively. Combining these with the P_V^i and P_T^i of the nonflipped part implies that the vector polarization should return from $-P_V^i$ to its initial value as Δf becomes smaller, while the tensor polarization should stay near P_T^i. This is observed in Figs. 6 and 7. Thus, the polarized deuteron behaves like a mixture of two polarized spin-1 fluids each obeying Eq. (4), one spin flipped and one unflipped, with the spin-flipped fraction decreasing as Δf decreases.

TABLE III. Fit results for Figs. 6 and 7 for $\Delta f/2 \geq 75$ Hz.

Vector and tensor fit results				
State	P_V^i	η_V	$\epsilon_V(\times 10^{-6})$	χ^2
$(-2/3, 0)$	-0.530 ± 0.022	1.00 ± 0.05	1.16 ± 0.03	5.6
$(-1/3, -1)$	-0.252 ± 0.015	1.20 ± 0.10	1.08 ± 0.04	4.5
$(-1, +1)$	-0.731 ± 0.029	0.93 ± 0.05	1.18 ± 0.03	0.8
$(+1, +1)$	0.741 ± 0.030	0.92 ± 0.05	1.19 ± 0.03	5.6
All states ($N - 2 = 30$)		0.973 ± 0.016	1.166 ± 0.010	36.0
State	P_T^i	η_T	$\epsilon_T(\times 10^{-6})$	χ^2
$(-1/3, -1)$	-0.50 ± 0.06	1.05 ± 0.05	1.14 ± 0.04	6.1
$(-1, +1)$	0.43 ± 0.08	1.03 ± 0.07	1.19 ± 0.06	1.0
$(+1, +1)$	0.61 ± 0.08	0.94 ± 0.04	1.16 ± 0.04	4.1
All states ($N - 2 = 22$)		0.988 ± 0.020	1.156 ± 0.027	22.7

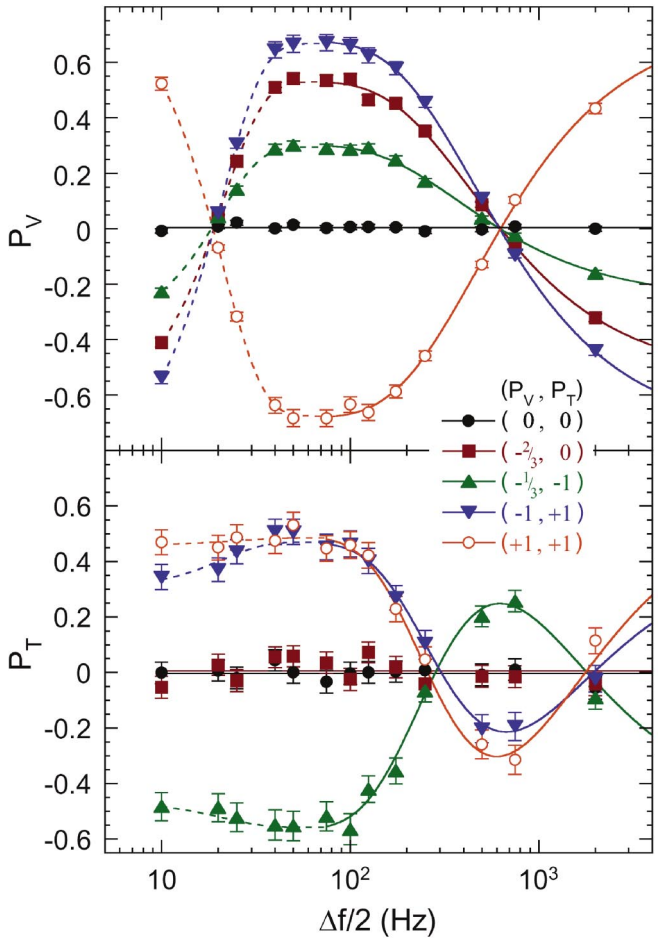

FIG. 6. (Color) The measured vector and tensor deuteron polarizations at 1850 MeV/c are plotted against the rf dipole's frequency half-range $\Delta f/2$. The rf dipole's ramp time Δt was 50 s, and its $\int B_{\rm rms} dl$ was 0.54 T mm. The top and bottom solid curves are fits to the data at and above $\Delta f/2 = 75$ Hz using Eqs. (9) and (11), respectively. The dashed lines are to guide the eye.

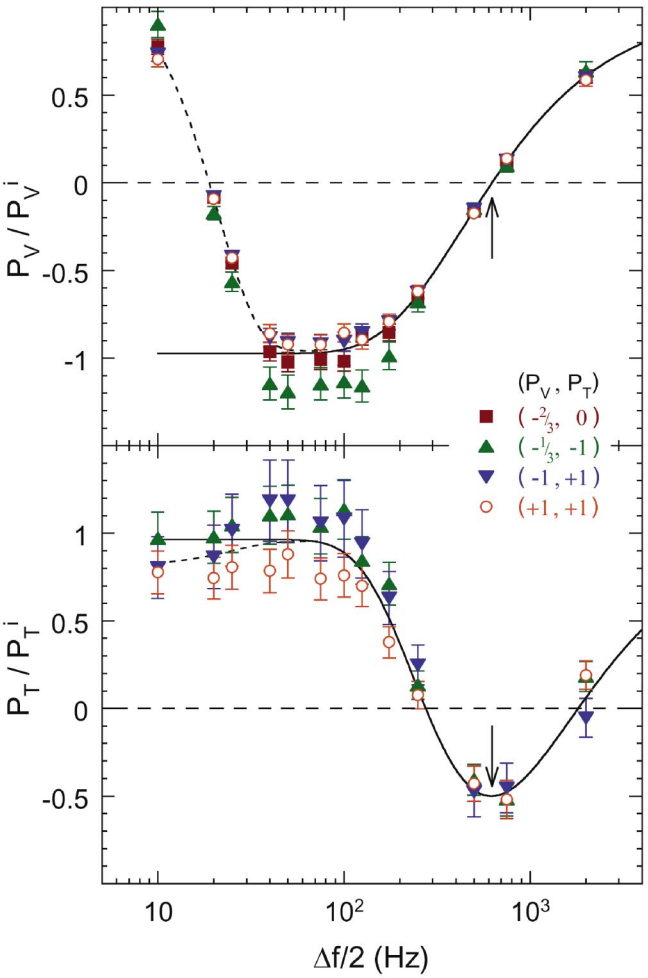

FIG. 7. (Color) The measured vector and tensor deuteron polarization ratios at 1850 MeV/c are plotted against the rf dipole's frequency half-range $\Delta f/2$. The P_V^i and P_T^i were obtained from fits to the data as shown in Table III. The rf dipole's ramp time Δt was 50 s, and its $\int B_{\rm rms} dl$ was 0.54 T mm. The top and bottom solid curves are fits to the data for all states at and above $\Delta f/2 = 75$ Hz using Eqs. (9) and (11), , respectively. The dashed lines are to guide the eye. The arrows mark a 90° rotation where $P_V = 0$ and $P_T = -\frac{1}{2} P_T^i$.

V. MULTIPLE SPIN FLIPPING

Using Figs. 5 and 7, we optimized the spin-flip efficiency by setting Δt at 60 s and Δf at 150 Hz at our maximum $\int B_{\rm rms} dl$. Then we more precisely determined the spin-flip efficiencies by simultaneously measuring, after n frequency sweeps, the vector and tensor polarizations P_V^n and P_T^n. To plot and fit these vector and tensor polarization data, we defined the *measured* spin-flip efficiencies η_V and η_T in terms of the measured P_V^n and P_T^n by taking the nth power of Eqs. (9) and (11):

$$P_V^n/P_V^i = (-\eta_V)^n; \quad P_T^n/P_T^i = \left[\frac{3}{2}(-\eta_T)^2 - \frac{1}{2}\right]^n. \quad (16)$$

We then calculated the ratios of the vector and tensor polarizations to their initial values; these ratios are plotted against n in Fig. 8 for the nonzero states. As indicated in Table IV, we fit these vector and tensor data using Eq. (16) to obtain

$$\eta_V = 96.5 \pm 0.6\%, \qquad \eta_T = 98.3 \pm 1.0\%, \quad (17)$$

for the data in Fig. 8. While these two values are close to each other, they are slightly outside of their statistical errors. Thus, in averaging them, we increased the error on their average by $\sqrt{\chi^2}$ to obtain a spin-flip efficiency

$$\eta = 97 \pm 1\%. \quad (18)$$

We also had a more recent run where we were able to flip the spin 5 times with rather good precision. There were some problems in calibrating the effective tensor analyzing powers, which may be resolved in a later paper. Thus, we only present the vector results at this time. These more recent vector data are plotted in Fig. 9. As indicated in

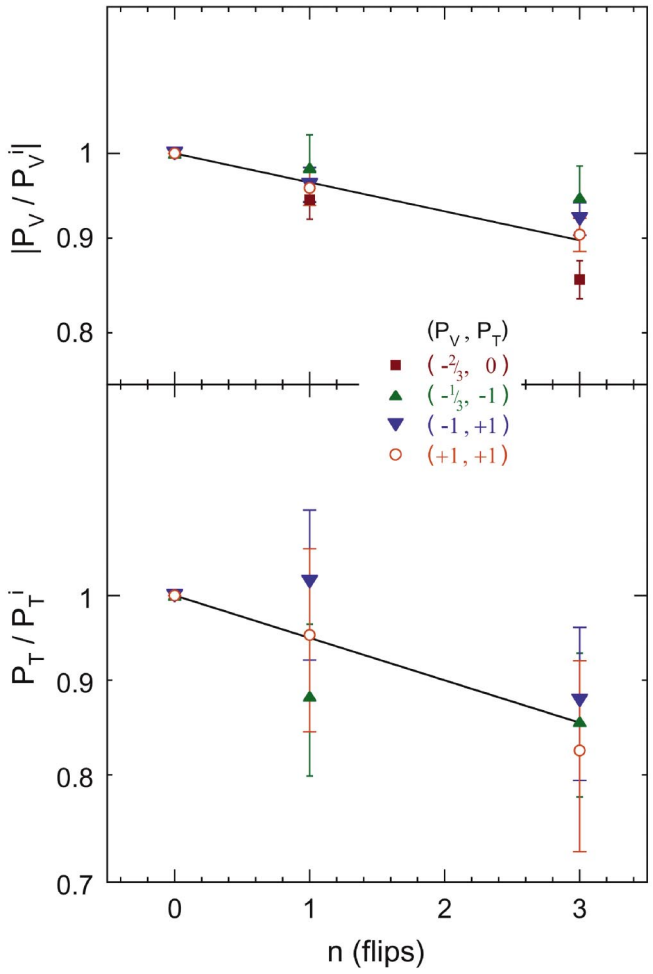

FIG. 8. (Color) The measured vector and tensor deuteron polarization ratios at 1850 MeV/c are plotted against the number of frequency sweeps. The rf dipole's frequency ramp time Δt was 60 s; its frequency half-range $\Delta f/2$ was 75 Hz, and its $\int B_{\rm rms} dl$ was 0.54 T mm. The lines are fits using Eq. (16).

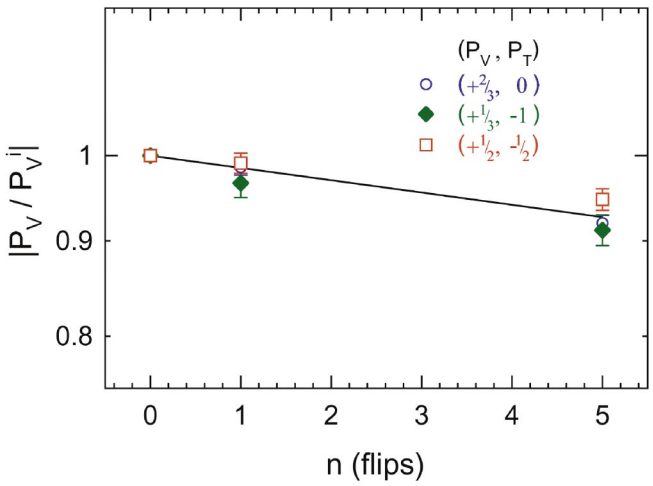

FIG. 9. (Color) The measured vector deuteron polarization ratios at 1850 MeV/c are plotted against the number of frequency sweeps. The rf dipole's frequency ramp time Δt was 60 s; its frequency half-range $\Delta f/2$ was 75 Hz, and its $\int B_{\rm rms} dl$ was 0.60 T mm. The line is a fit using Eq. (16).

TABLE IV. Fit results for Figs. 8 and 9.

Vector and tensor fit results		
State	η_V	χ^2
All states in Fig. 8 ($N-1=7$)	0.965 ± 0.006	9.1
All states in Fig. 9 ($N-1=5$)	0.985 ± 0.003	5.4
State	η_T	χ^2
All states in Fig. 8 ($N-1=5$)	0.983 ± 0.010	1.4

Table IV, we fit them to Eq. (16) to obtain

$$\eta_V = 98.5 \pm 0.3\%. \tag{19}$$

Since the tensor calibration problem might cause some small second-order changes in η_V, we increased the error from its statistical value of 0.2% to 0.3%.

VI. SUMMARY

By adiabatically sweeping an rf dipole's frequency through an rf-induced spin resonance, we spin-manipulated the vector and tensor polarizations of a vertically polarized 1.85 GeV/c spin-1 deuteron beam. We experimentally demonstrated that a single spin-flip efficiency η and a single resonance strength ϵ can describe both the vector and tensor polarizations. Their interesting behavior, first seen at IUCF [15] and now confirmed at COSY, can be understood in terms of the quantum mechanics of spin-1 rotations, Eq. (4), and the Froissart-Stora equation, Eq. (5).

By decreasing the frequency sweep range Δf, we found that the Froissart-Stora equation became invalid, as expected, when Δf was not significantly larger than the resonance width w. However, the behavior of the vector and tensor polarizations in this small Δf region can be described in terms of a simple model of a mixture of two polarized spin-1 fluids each obeying Eq. (4); one is spin flipped and one is unflipped, with the spin-flipped fraction decreasing as Δf decreases.

Multiple spin flips were used to determine more precisely the spin-flip efficiency η of both the vector and tensor polarizations. By placing the spin-resonance crossing parameters, Δf and Δt, at their optimal values, we reached a measured spin-flip efficiency of $97 \pm 1\%$ and $98.5 \pm 0.3\%$ for two separate runs with 1.85 GeV/c vertically polarized spin-1 deuterons stored in the COSY ring. These were significantly higher than the $94.2 \pm 0.3\%$ attained at IUCF [15].

ACKNOWLEDGMENTS

We would like to thank the entire COSY staff for the successful operation of COSY with its injector cyclotron and polarized ion source. We are grateful to A. W. Chao, E. D. Courant, Ya. S. Derbenev, G. Fidecaro, W. Haeberli, H. Huang, T. Roser, H. Sato, W. Scobel, and others for their help and advice. This research was supported by grants from the German BMBF Science Ministry.

[1] R. Alarcon *et al.* (BLAST Collaboration), in MIT Bates Report No. 2-39, 1999.

[2] H. Rohdjess *et al.*, in *SPIN 2002: 15th International Spin Physics Symposium and Workshop on Polarized Electron Sources and Polarimeters, Upton, NY, 2002*, edited by Y. I. Makdisi *et al.*, AIP Conf. Proc. No. 675 (AIP, Melville, NY, 2003), p. 523.

[3] Y. Makdisi, in *High Energy Spin Physics: 11th International Symposium, Bloomington, IN, 1994*, edited by Kenneth J. Heller and Sandra L. Smith, AIP Conf. Proc. No. 343 (AIP, Woodbury, NY, 1995), p. 75.

[4] A. D. Krisch *et al.* (SPIN Collaboration), University of Michigan Report No. UM-HE 96-20, 1996; University of Michigan Report No. UM-HE 99-05, 1999.

[5] A. Airapetian *et al.* (HERMES Collaboration), DESY-PRC Report No. 99-08, 1999.

[6] V. S. Morozov *et al.*, Phys. Rev. ST Accel. Beams **4**, 104002 (2001).

[7] D. D. Caussyn *et al.*, Phys. Rev. Lett. **73**, 2857 (1994).

[8] D. A. Crandell *et al.*, Phys. Rev. Lett. **77**, 1763 (1996).

[9] B. B. Blinov *et al.*, Phys. Rev. Lett. **81**, 2906 (1998); V. A. Anferov *et al.*, in *Proceedings of the 13th International Symposium on High Energy Spin Physics (IHEP), Protvino, Russia, 1998*, edited by N. E. Tyurin *et al.* (World Scientific, Singapore, 1999), p. 503.

[10] V. A. Anferov *et al.*, Phys. Rev. ST Accel. Beams **3**, 041001 (2000).

[11] B. B. Blinov *et al.*, Phys. Rev. ST Accel. Beams **3**, 104001 (2000).

[12] A. M. T. Lin *et al.*, in *SPIN 2000: 14th International Spin Physics Symposium*, edited by K. Hatanaka, AIP Conf. Proc. No. 570 (AIP, Melville, NY, 2001), p. 736.

[13] B. B. Blinov *et al.*, Phys. Rev. Lett. **88**, 014801 (2002).

[14] V. S. Morozov *et al.*, Phys. Rev. ST Accel. Beams **7**, 024002 (2004).

[15] V. S. Morozov *et al.*, Phys. Rev. Lett. **91**, 214801 (2003).

[16] *Madison Convention, Proceedings of the 3rd International Symposium on Polarization Phenomena in Nuclear Physics, Madison, 1970*, edited by H. H. Barschall and W. Haeberli (University of Wisconsin Press, Madison, WS, 1971), p. xxv.

[17] H. Huang *et al.*, in *Proceedings of the 1993 Particle Accelerator Conference, Washington, DC, 1993*, edited by S. T. Corneliussen (IEEE, Piscataway, NJ, 1993), p. 432.

[18] B. W. Montague, Phys. Rep. **113**, 35 (1984).

[19] M. Froissart and R. Stora, Nucl. Instrum. Methods **7**, 297 (1960).

[20] There is a factor of 2 disagreement between the two below references for Eq. (6); this disagreement has no effect on our results. T. Roser, *Handbook of Accelerator Physics and Engineering*, edited by A. Chao and M. Tigner (World Scientific, Singapore, 2002), p. 153, Eq. (7). H. Stockhorst and B. Lorentz, COSY internal report, 2003 (unpublished).

[21] R. Maier, Nucl. Instrum. Methods Phys. Res., Sect. A **390**, 1 (1997).

[22] A. Lehrach *et al.*, in *Proceedings of the 1999 Particle Accelerator Conference, New York, NY, 1999*, edited by A. Luccio and W. MacKay (IEEE, Piscataway, NJ, 1999), p. 2292.

[23] H. Stockhorst *et al.*, in *Proceedings of the 8th European Particle Accelerator Conference, Paris, 2002* (EPS-IGA/CERN, Geneva, 2002), p. 629.

[24] A. Lehrach *et al.*, in *SPIN 2002: 15th International Spin Physics Symposium and Workshop on Polarized Electron Sources and Polarimeters, Upton, NY, 2002* (Ref. [2]), p. 153.

[25] M. Altmeier *et al.* (EDDA Collaboration), Phys. Rev. Lett. **85**, 1819 (2000).

[26] P. D. Eversheim *et al.*, in *Proceedings of the 8th International Symposium on Polarization Phenomena in Nuclear Physics, Bloomington, IN, 1994*, edited by Edward J. Stephenson and Steven E. Vigdor, AIP Conf. Proc. No. 339 (AIP, Woodbury, NY, 1995), p. 668.

[27] R. Weidmann *et al.*, Rev. Sci. Instrum. **67**, 1357 (1996).

[28] O. Felden *et al.*, in *Proceedings of the 9th International Workshop on Polarized Sources and Targets, Nashville, IN, 2001*, edited by V. P. Derenchuk and B. von Przewoski (World Scientific, Singapore, 2002), p. 200.

[29] K. Yonehara *et al.*, in *Proceedings of the 8th Conference on the Intersections of Particle and Nuclear Physics, New York, NY, 2003*, edited by Z. Parsa, AIP Conf. Proc. No. 698 (AIP, Melville, NY, 2003), p. 763.

[30] B. von Przewoski *et al.*, Rev. Sci. Instrum. **67**, 165 (1996).

[31] J. E. Goodwin *et al.*, Phys. Rev. Lett. **64**, 2779 (1990).

[32] V. A. Anferov *et al.*, Phys. Rev. A **46**, R7383 (1992).

[33] H. Rohdjess, SPIN@COSY internal report, 2004 (unpublished).

[34] K. Sekiguchi *et al.*, Phys. Rev. C **65**, 034003 (2002).

[35] M. Haji-Saied *et al.*, Phys. Rev. C **36**, 2010 (1987).

[36] V. S. Morozov, SPIN@COSY internal report, 2004 (unpublished).